Electronic Supplementary Information (ESI)

Two ultramicroporous metal-organic frameworks assembled from binuclear secondary building units for highly selective CO_2/N_2 separation

Shuang Liu,[a] Shuo Yao,[b] Bing Liu,[a] Xiaodong Sun,[a] Yang Yuan,[a] Guanghua Li,[a] Lirong Zhang,*[a] and Yunling Liu*[a]

[a.] State Key Laboratory of Inorganic Synthesis and Preparative Chemistry, College of Chemistry, Jilin University, Changchun 130012, P. R. China.

E-mail: yunling@jlu.edu.cn; Fax: +86-431-85168624; Tel: +86-431-85168614

[b.] Key Laboratory of Marine Chemistry Theory and Technology, Ministry of Education, Ocean University of China, Songling Road 238, Qingdao 266100, China.

E-mail: yaoshuo@ouc.edu.cn

S1. Calculation procedures of selectivity from IAST

The measured experimental data is excess loadings (q^{ex}) of the pure components CO_2, for **JLU-MOF56** and **JLU-MOF57**, which should be converted to absolute loadings (q) firstly.

$$q = q^{ex} + \frac{pV_{pore}}{ZRT}$$

Here Z is the compressibility factor. The Peng-Robinson equation was used to estimate the value of compressibility factor to obtain the absolute loading, while the measure pore volume 0.708 $cm^3\ g^{-1}$ and 0.804 are also necessary.

The dual-site Langmuir-Freundlich equation is used for fitting the isotherm data at 298K.

$$q = q_{m_1} \times \frac{b_1 \times p^{1/n_1}}{1 + b_1 \times p^{1/n_1}} + q_{m_2} \times \frac{b_2 \times p^{1/n_2}}{1 + b_2 \times p^{1/n_2}}$$

Here p is the pressure of the bulk gas at equilibrium with the adsorbed phase (kPa), q is the adsorbed amount per mass of adsorbent (mol kg^{-1}), q_{m1} and q_{m2} are the saturation capacities of sites 1 and 2 (mol kg^{-1}), b_1 and b_2 are the affinity coefficients of sites 1 and 2 (1/kPa), n_1 and n_2 are the deviations from an ideal homogeneous surface.

The selectivity of preferential adsorption of component 1 over component 2 in a mixture containing 1 and 2, perhaps in the presence of other components too, can be formally defined as q_1 and q_2 are the

$$S = \frac{q_1/q_2}{p_1/p_2}$$

absolute component loadings of the adsorbed phase in the mixture. These component loadings are also termed the uptake capacities. We calculate the values of q_1 and q_2 using the Ideal Adsorbed Solution Theory (IAST) of Myers and Prausnitz.

S2. Supporting Figures

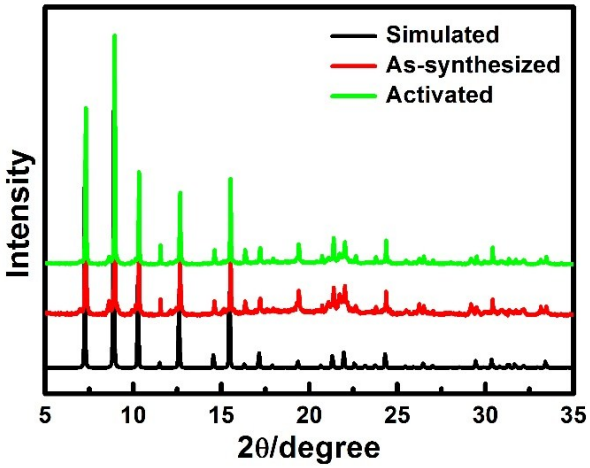

Fig. S1. PXRD patterns of **JLU-MOF56** for simulated, as-synthesized and activated samples. The differences in reflection intensity are probably due to preferred orientations in the powder sample.

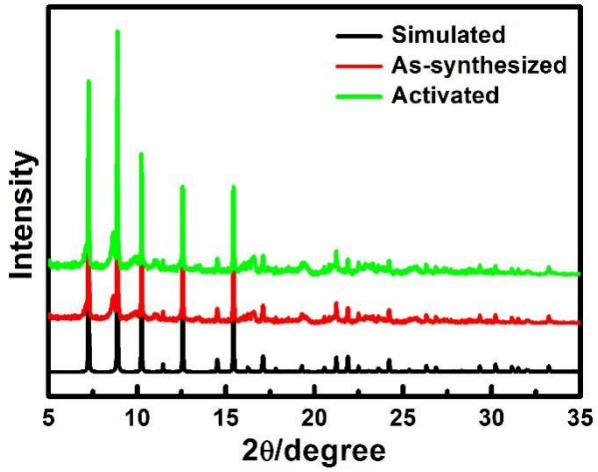

Fig. S2. PXRD patterns of **JLU-MOF57** for simulated, as-synthesized and activated samples. The differences in reflection intensity are probably due to preferred orientations in the powder sample.

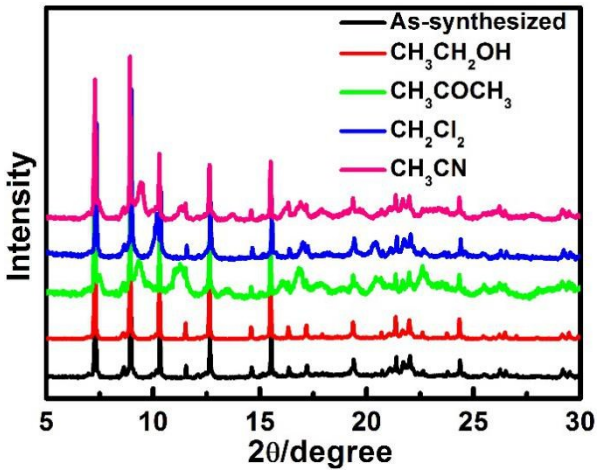

Fig. S3. PXRD patterns of **JLU-MOF56** samples for as-synthesized and immersed in different organic solutions at room temperature.

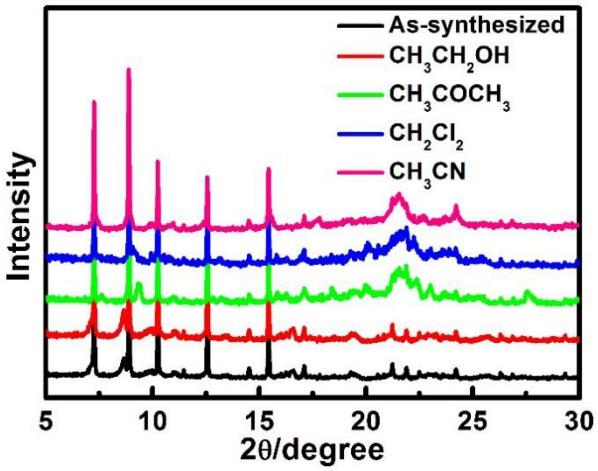

Fig. S4. PXRD patterns of **JLU-MOF57** samples for as-synthesized and immersed in different organic solutions at room temperature.

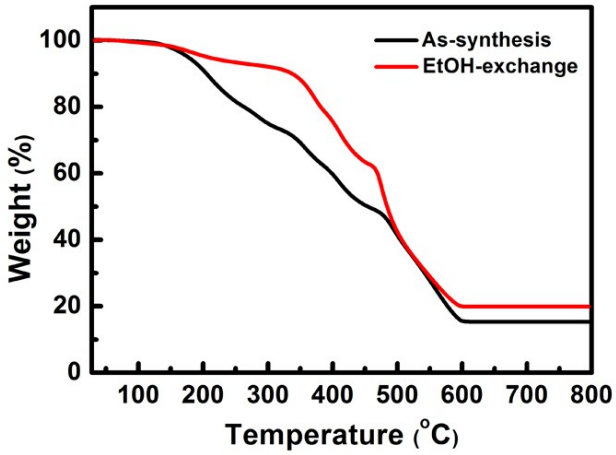

Fig. S5. Thermogravimetric analysis curves of **JLU-MOF56** for the as-synthesized and EtOH exchanged samples.

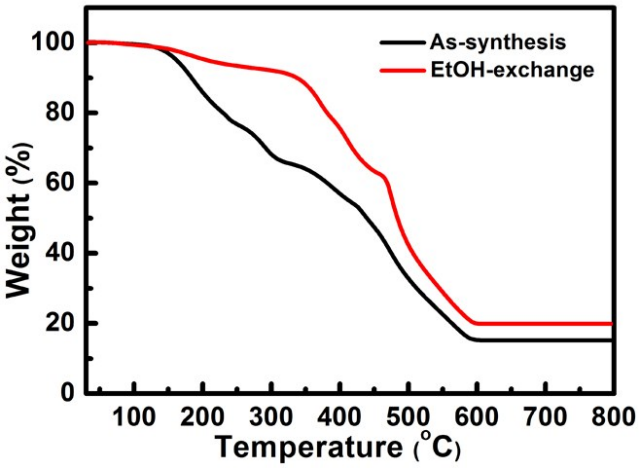

Fig. S6. Thermogravimetric analysis curves of **JLU-MOF57** for the as-synthesized and EtOH exchanged samples.

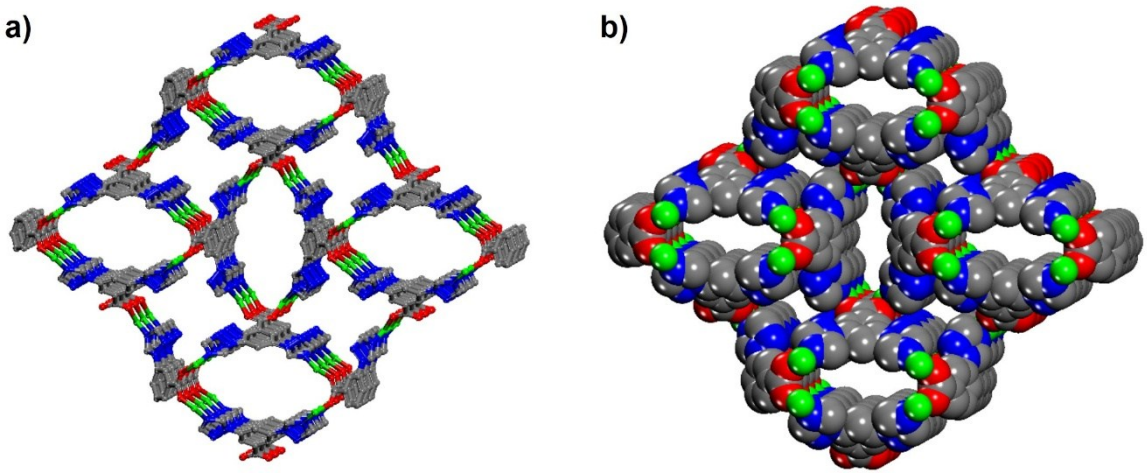

Fig. S7. The stick model (a) and the CPK model (b) of the channel along the [010] direction.

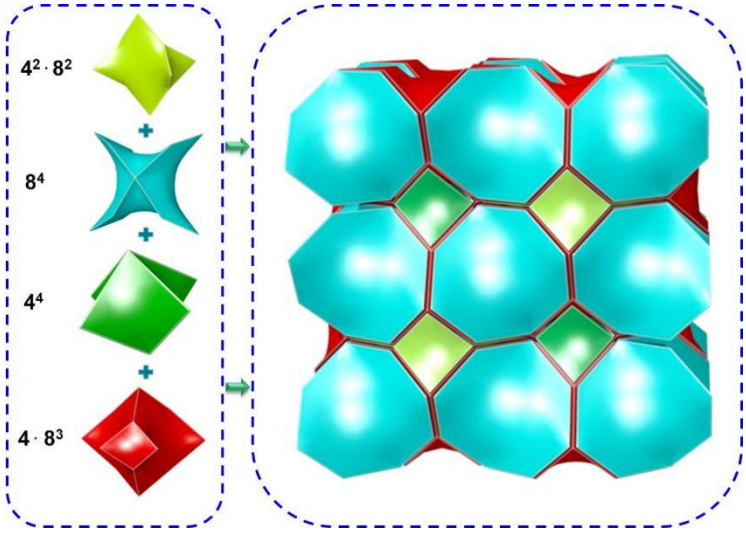

Fig. S8. Topological features of **JLU-MOF56** and **JLU-MOF57** displayed by tiles and face symbols for yellow blue, green and red tiles are $\{4^2.8^2\}$, $\{8^4\}$, $\{4^4\}$ and $\{4.8^3\}$.

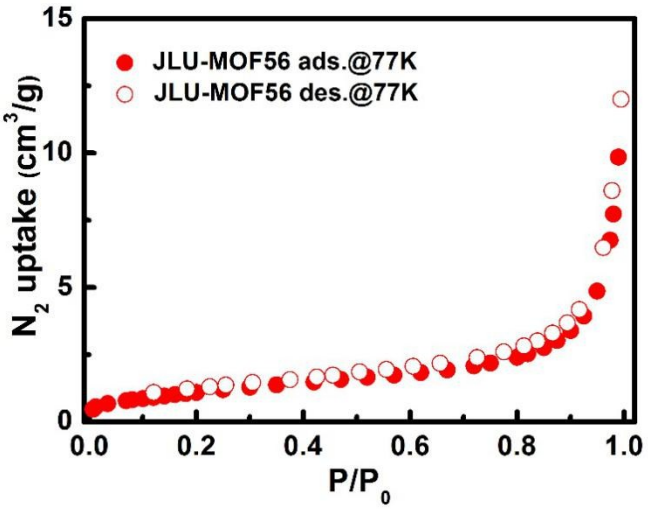

Fig. S9. The N_2 isotherm for **JLU-Liu56** at 77 K under 1 bar.

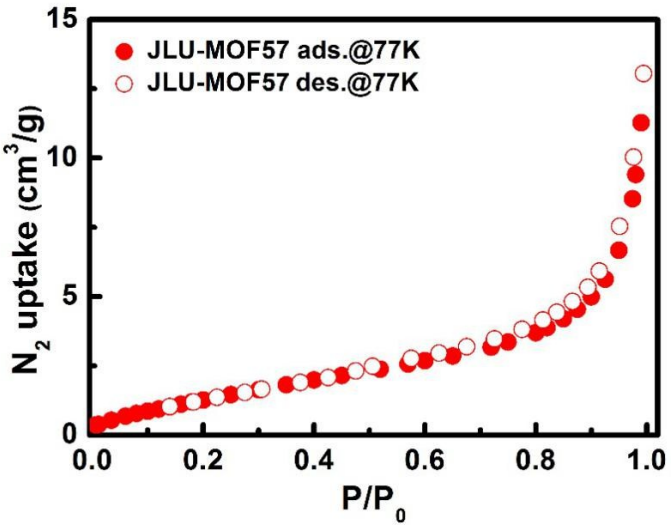

Fig. S10. The N_2 isotherm for **JLU-MOF57** at 77 K under 1 bar.

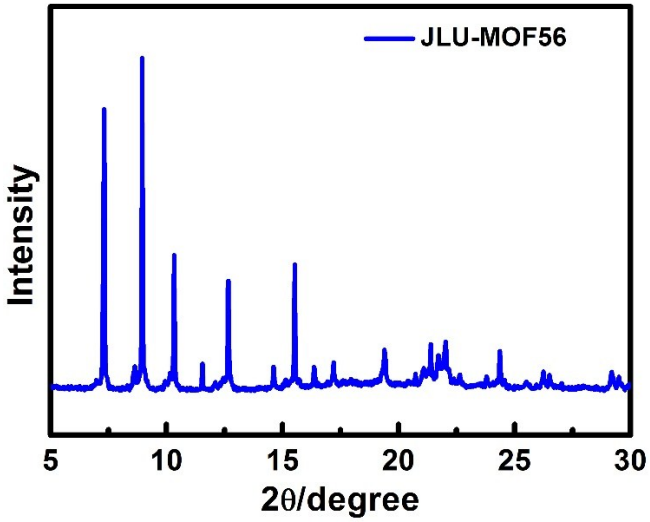

Fig. S11. PXRD pattern of **JLU-MOF56** samples after the CO_2 adsorption.

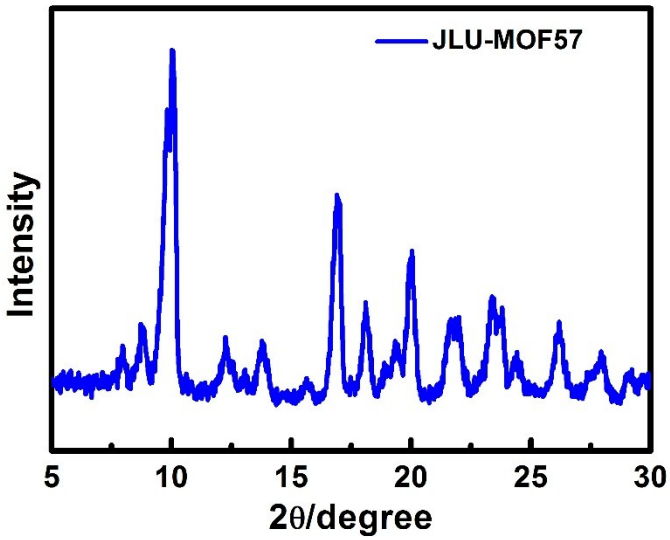

Fig. S12. PXRD pattern of **JLU-MOF57** samples after the CO_2 adsorption.

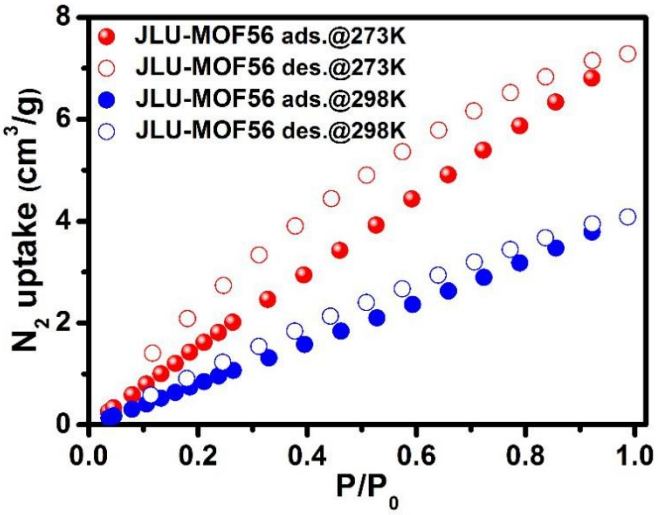

Fig. S13. The N_2 isotherm for **JLU-MOF56** at 273 K and 298 K under 1 bar.

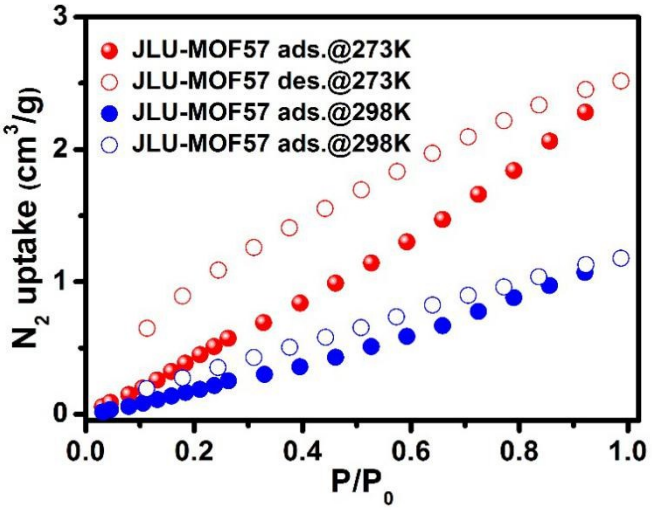

Fig. S14. The N_2 isotherm for **JLU-MOF57** at 273 K and 298 K under 1 bar.

Table S1. Crystal data and structure refinements for JLU- MOF56 and JLU- MOF57

compound	**JLU-MOF56**	**JLU-MOF57**
formula	$C_{37}H_{49}Cl_2N_{17}Ni_2O_9$	$C_{37}H_{49}Cl_2N_{17}Co_2O_9$
Mw	1064.25	1064.69
temp (K)	293(2)	293(2)
wavelength (Å)	0.71073	0.71073
Crystal system	Tetragonal	Tetragonal
space group	P4(2)/mnm	P4(2)/mnm
a (Å)	17.031(2)	17.274(2)
b (Å)	17.031(2)	17.274(2)
c (Å)	17.184(3)	17.178(3)
V (Å^3)	4984.3(14)	5125.6(14)
Z, D_c (Mg/m^3)	4, 1.418	4, 1.323
F(000)	2208.0	2200
θ range (deg)	2.91-27.47	1.67-25.15
reflns collected/unique	56827/3088	32057/2496
R_{int}	0.0376	0.0440
data/restraints/params	3088/67/133	2496/27/125
GOF on F^2	1.066	1.103
R_1, wR_2 (I>2σ(I))	0.0486, 0.1411	0.0464,0.1419
R_1, wR_2 (all data)	0.0520, 0.1439	0.0535,0.1462

[a] $R_1 = \Sigma||F_o| - |F_c||/\Sigma|F_o|$, [b] $wR_2 = [\Sigma w(|F_o|^2 - |F_c|^2)/\Sigma|w(F_o^2)^2|]^{1/2}$

Table S2. Selected bond lengths [Å] and angles [º] for **JLU-MOF56**.

JLU- MOF56			
Ni(1)-O(1)#1	2.0319(17)	O(1)#2-Ni(1)-N(3)	86.51(9)
Ni(1)-O(1)#2	2.0319(17)	O(1)#1-Ni(1)-N(3)#3	86.51(9)
Ni(1)-N(3)	2.087(2)	O(1)#2-Ni(1)-N(3)#3	173.01(8)
Ni(1)-N(3)#3	2.087(2)	N(3)-Ni(1)-N(3)#3	92.59(13)
Ni(1)-O(2)	2.122(3)	O(1)#1-Ni(1)-O(2)	85.29(8)
Ni(1)-Cl(1)	2.3963(9)	N(3)-Ni(1)-O(2)	87.75(8)
O(1)-C(7)	1.246(2)	N(3)#3-Ni(1)-O(2)	87.75(8)
O(1)-Ni(1)#5	2.0319(17)	O(1)#1-Ni(1)-Cl(1)	96.80(6)
O(2)-C(8)	1.267(12)	N(3)-Ni(1)-Cl(1)	90.14(6)
N(1)-C(5)	1.330(3)	O(2)-Ni(1)-Cl(1)	176.94(8)
N(1)-N(2)	1.386(14)	Ni(1)#4-Cl(1)-Ni(1)	99.12(5)
N(1)-C(2)	1.428(3)	C(7)-O(1)-Ni(1)#5	136.25(19)
O(1)#1-Ni(1)-O(1)#2	93.55(11)	C(8)#3-O(2)-Ni(1)	119.4(7)
O(1)#1-Ni(1)-N(3)	173.01(8)	C(8)-O(2)-Ni(1)	94.38(4)

Symmetry transformations used to generate equivalent atoms:
#1 -y+3/2,x-1/2,z-1/2 #2 -y+3/2,x-1/2,-z+1/2 #3 x,y,-z #4 -y+1,-x+1,z #5 y+1/2,-x+3/2,-z+1/2 #6 y,x,z

Table S3. Selected bond lengths [Å] and angles [º] for **JLU-MOF57**.

JLU-MOF57			
Co(1)-O(1)#1	2.0561(19)	O(1)#1-Co(1)-O(1)#2	94.36(12)
Co(1)-O(1)#2	2.0561(19)	O(1)#1-Co(1)-N(3)#3	172.72(10)
Co(1)-N(3)#3	2.141(3)	O(1)#2-Co(1)-N(3)#3	86.66(10)
Co(1)-N(3)	2.141(3)	O(1)#1-Co(1)-N(3)	86.66(10)
Co(1)-O(2)	2.160(3)	O(1)#2-Co(1)-N(3)	172.72(10)
Co(1)-Cl(1)	2.4351(12)	N(3)#3-Co(1)-N(3)	91.44(15)
Cl(1)-Co(1)#4	2.4351(12)	O(1)#1-Co(1)-O(2)	85.86(9)
O(1)-C(7)	1.246(3)	O(1)#2-Co(1)-O(2)	85.86(9)
O(1)-Co(1)#5	2.0561(19)	N(3)#3-Co(1)-O(2)	87.03(10)
O(2)-C(8)	1.145(14)	N(3)-Co(1)-O(2)	87.03(10)
N(1)-C(5)	1.325(4)	O(1)#1-Co(1)-Cl(1)	97.26(6)
N(1)-N(2)	1.359(4)	O(1)#2-Co(1)-Cl(1)	97.26(6)
N(1)-C(2)	1.433(4)	N(3)#3-Co(1)-Cl(1)	89.75(8)
N(2)-C(6)	1.305(5)	N(3)-Co(1)-Cl(1)	89.75(8)
N(3)-C(5)	1.311(4)	O(2)-Co(1)-Cl(1)	175.38(10)
N(3)-C(6)	1.342(4)	Co(1)-Cl(1)-Co(1)#4	97.35(6)

Symmetry transformations used to generate equivalent atoms:
#1 -y+1/2,x+1/2,-z+1/2 #2 -y+1/2,x+1/2,z-1/2 #3 x,y,-z #4 y,x,-z #5 y-1/2,-x+1/2,-z+1/2 #6 -y,-x,z

Table S4. CO_2/N_2 separation selectivity for reported MOFs materials at 1 bar.

Compound	CO_2/N_2	Temperature (K)	Ref.
Bio-MOF-11	79.5	296	1
Cu-TDPAT	57.8	296	1
IITKGP-8	43.7	295	2
UTSA-72a	35.6	296	3
JLU-MOF56	32.8	298	This work
TIFSIX-1-Cu	30	298	4
HKUST-1(hydrated)	28	298	5
JUC-141	27.60	298	6
SIFSIX-1-Cu	27	298	7
PMOF-3a	23.4	296	8
$Cu_{24}(TPBTM)_8$	22	298	9
Cu-BTTri	21	298	10
JLU-MOF57	20.3	298	This work
PCN-88	18	296	11
PCN-61	15	298	12
ZJNU-44a	15	296	9
SIFSIX-2-Cu	13.7	298	7
MOF-177	3.6	296	1

Reference:

1. S. Xiang, Y. He, Z. Zhang, H. Wu, W. Zhou, R. Krishna and B. Chen, *Nat. Commun.*, 2012, **3**, 954–963.
2. S. Chand, A. Pal and M. Das, *Chem. Euro. Jour.*, 2018, **24**, 5982-5986.
3. H. Alawisi, B. Li, Y. He, H. Arman, A. Asiri, H. Wang and B. Chen, *Cryst.Growth. Des.*, 2014, **14**, 2522–2526.
4. P. Nugent, V. Rhodus, T. Pham, B.Tudor, K. Forrest, L. Wojtas, B. Space and M. Zaworotko, *Chem. Commun.*, 2013, **49**,1606–1608.
5. A. Yazaydın, A. Benin, S. Faheem, P. Jakubczak, J. Low, R. Willis and R. Snurr, *Chem. Mater.*, 2009, **21**, 1425–1430.
6. N. Zhao, F. Sun, P. Li, X. Mu, G. Zhu, *Inorg. Chem.*, 2017, **56**, 6938–6942.
7. P. Nugent, Y. Belmabkhout, S. Burd, A. Cairns, R. Luebke, K. Forrest, T. Pham, S. Ma, B. Space, L. Wojtas, M. Eddaoudi and M. Zaworotko, *Nature.*, 2013, **495**, 80–84.
8. O. Alduhaish, H. Wang, B. Li, T. Hu, H. Arman, K. Alfooty and B. Chen, *Chem. Plus. Chem.*, 2016, **81**, 770–774.

9. C. Song, J. Hu, Y. Ling, Y. Feng, R. Krishna, D. Chen and Y. He, *J. Mater. Chem. A.*, 2015, **3**, 19417–19426.
10. A. Demessence, D. Alessandro, M. Foo and J. Long, *J. Am. Chem. Soc.*, 2009, **131**, 8784–8786.
11. J. Li, J. Yu,W. Lu, L. Sun, J. Sculley, P. Balbuena and H.-C. Zhou, *Nat. Commun.*, 2013, **4**, 204–212.
12. B. Zheng, J. Bai, J. Duan, L. Wojtas and M. Zaworotko, *J. Am. Chem. Soc.*, 2011, **133**, 748–751.